

## STUDY OF OXIDE FILMS FORMED ON IRIIDIUM IMPLANTED Ti-6Al-4V ALLOY

T. M. Silva, M. G. S. Ferreira\*, M. da Cunha Belo

*Instituto Superior Técnico, Dep. Engenharia Química, Av. Rovisco Pais, 1096 Lisboa Codex, Portugal*

### Abstract

The oxide films formed by potential cycling on commercial Ti6Al4V alloy, that has been surface implanted with iridium, are studied by capacitance measurements and Auger analysis. It is observed that these films become enriched in iridium when etched in sulphuric acid solution prior to their formation, simultaneously with a change in the type of semiconductivity (n-type to p-type).

### Keywords

Iridium Oxide, Ion Implantation, Auger, Capacitance Measurements, Semiconductive Films

### Introduction

The development of electronic devices for biomedical applications has been, in recent years, a very active area. Among these devices are the neural stimulating electrodes, which interface directly to the nervous system and are used to replace or supplementing function in the neurological handicapped [1-3].

Artificial stimulation of the nervous system requires the transfer of a certain amount of charge (typically  $10\text{mC}/\text{cm}^2$  in the case of auditory prostheses [4]) from the electrode to the nerve cells, which can be accomplished by electrochemical processes occurring at the electrode/solution interface. Irreversible faradaic reactions, such as metallic corrosion or gas evolution, leading to the introduction of new species in the physiological medium, should be avoided as these new species can be potentially harmful to the neighbour tissues [5].

Safe stimulation of the nervous system requires therefore a reversible charge transfer process. Capacitive electrodes, in which charge is stored across a dielectric film, is one possible way to provide nerve stimulation. However, only a limited amount of charge, generally  $20\text{-}30\ \mu\text{C}/\text{cm}^2$ , is passed while the double layer is charging [3,6]. For that reason as an alternative, charge transfer based on reversible faradaic reactions has been investigated. These electrodes allow improved charge storage capacity through a fast and reversible redox reaction involving species that remain bound to the surface [5]. Iridium oxide is one of the most promising materials to be used in these

electrodes since, for a given applied potential pulse, it injects the highest charge density of any known material [3, 6,7].

It has been known for a few years that thick iridium oxide films, presenting a highly hydrated [8] and porous nature [9-11], can easily be grown on a pure Ir substrate by cycling the potential between a sufficiently negative and positive potential [12]. The charge storage capacity of the oxide is directly related with its thickness and it is mainly associated with a highly reversible redox reaction in which the oxidation state of Ir ions changes between III and IV [10,13,14]. Simultaneously with this redox process, ion transfer across the film/solution interface occurs in order to neutralise space-charge effects associated with the addition/withdrawal of electrons, being however the nature of the ions still controversial [12,15-17].

Oxidation of Ir(III) is accompanied by a four orders of magnitude increase in the electrical conductivity of the material [18] and an electrochromic effect in which the oxide changes from colourless to blue-black [12,16]. The aforementioned effects are reversible on cycling between Ir(III) and Ir(IV) states.

Besides the good charge injection capability presented by neuro-stimulating electrodes, they should be reduced to the size of neurones and placed as close to them as possible, avoiding in this way the lack of selectivity in neuronal activation. Although iridium oxide possesses the required charge injection properties, iridium is very brittle and therefore difficult to fabricate into microelectrodes [1].

The present study is the continuation of a work in which evaluation of the charge storage properties of Ir ion implanted Ti-6Al-4V alloy was carried out [19]. The ion implantation technique was chosen as it offers the capability of introducing a small amount of the noble material without modifying the surface finishing or affecting bulk physical and mechanical properties. In this way an attempt was made to combine the good mechanical properties of the Ti-alloy substrate with the electrochemical properties of the Ir oxide. It was shown that, if the implanted alloy is submitted to an adequate chemical treatment, the charge storage capacity of the electrodes is sufficient for some types of neural stimulating electrodes. In this work the chemical composition of the oxide films, formed by cyclic voltammetry, on the implanted and etched samples was controlled by Auger depth profiling. Capacitance measurements (Mott-Schottky approach) were also performed in order to obtain a better understanding of the electronic structure of the oxides.

### Experimental

Iridium was ion implanted on commercial Ti-6Al-4V alloy (Goodfellow), at energy of 20keV and with a fluency of  $1 \times 10^{17}$  ions/cm<sup>2</sup>. The specimens have been previously polished to 1  $\mu$ m

diamond paste. After ion implantation, chemical etching of the samples was made by immersion in deaerated 70% H<sub>2</sub>SO<sub>4</sub> at room temperature.

Iridium oxide films were grown on the implanted substrate by cycling the potential at a scan rate of 0.1V/sec between -0.65V and 0.85V (vs. SCE), using an AUTOLAB PGSTAT potentiostat. These potentials were chosen since decomposition of the solution occurs outside this range.

Capacitance results were obtained by a.c. measurements using a sinusoidal perturbing amplitude of 10mV with a frequency of 1kHz. Measurements were performed in a potential range of -0.8V to 0.7V at intervals of 0.05V. The experiments were performed using a 273EG&G potentiostat and a 5210 EG&G lock-in amplifier.

All the electrochemical measurements were performed in a conventional three-electrode cell using a Pt wire as counter-electrode and a saturated calomel electrode as reference. Potentials are therefore quoted with respect to SCE. In order to reproduce the physiological environment all experiments were conducted in 0.1M Na<sub>2</sub>HPO<sub>4</sub> + 0.1M KH<sub>2</sub>PO<sub>4</sub> buffer solution at pH 6.9 under continuous N<sub>2</sub>-bubbling.

The chemical composition of the films was investigated by Auger electron spectroscopy (AES), using a MICROLAB 310-F (VG SCIENTIFIC) equipped with a concentric hemispherical analyser, using 10keV, 50nA electron beam with a diameter of ~75nm. Depth profiling was performed by sputtering the sample with an Ar<sup>+</sup> ion beam with a current of 0.5-0.8  $\mu$ A/mm<sup>2</sup> and an acceleration voltage of 1keV.

Secondary ion mass spectrometry (SIMS) analysis has been performed on the as-implanted samples by a CAMECA ims-4f microscope. A 14.5keV Cs<sup>+</sup> primary beam, focused to about 5 $\mu$ m diameter, was rastered over an area of 250x250 $\mu$ m<sup>2</sup> and the secondary positive ions, emitted from a central circular area (20 $\mu$ m diameter) were collected by the spectrometer.

### Results and Discussion

Fig. 1 shows the near-gaussian implant profile of Ir, measured by SIMS. The peak concentration is located about 15nm below the surface and the implanted zone presents a thickness of ~80nm. The surface Ir concentration is typically very small. Therefore, it is expectable that the behaviour of the implanted material would resemble that of the Ti-alloy substrate, with low values of charge storage capacity, making the material non-suitable for using as a neural-stimulating electrode.

For this reason, after ion implantation, the electrodes were subjected to selective dissolution of the substrate by means of immersion in an etching solution. As the dissolution of Ti occurs,

subsequent build-up and retention of surface iridium is expected, making it possible to obtain a material presenting high Ir surface concentration. Such a process was shown to be effective for Ti implanted with Pd, Pt, and Ru [20,21].

A solution of 70% H<sub>2</sub>SO<sub>4</sub> was chosen since the Ti-alloy dissolves quickly there. None of the alloy components becomes passivated in the solution as shown by the open-circuit potential measurements performed in previous work [19].

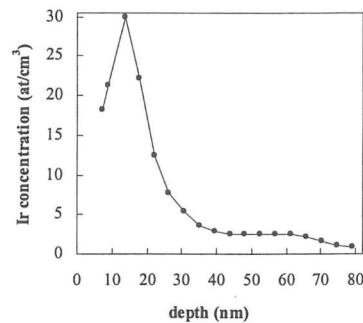


Fig. 1 - Typical Ir concentration depth profile determined by SIMS.

In order to select the best conditions for the enrichment process several immersion periods were tested. Subsequently Ir oxide films were grown on the etched samples by applying 100 potential cycles, and the so-formed oxide film was analysed by AES depth profiling.

*Electrochemical Testing*

Anodically formed iridium oxide films have been extensively studied by several authors in different solutions [22-26] and it is generally accepted that the oxide composition is essentially the same despite the solution used in the growing process.

For comparison purposes, voltammograms of the oxides formed after 100 potential cycles in the two limiting cases i.e., on a pure iridium substrate and on the unimplanted Ti-alloy, are shown in Fig. 2.

As expected, and reversely to the case of the iridium electrode, the unimplanted Ti-alloy shows no evidence of charge storage capacity, as revealed by the low value of the area under the voltammogram.

In the case of iridium oxide, as mentioned above, the high storage capacity presented by the material has been related to a valence change from Ir<sup>3+</sup> to Ir<sup>4+</sup> [10,13,14], which is evidenced in the

current peak depicted at ~0.1V. It is also well known that repetitive potential cycling enhances this property due to continuous Ir oxide growth at the surface.

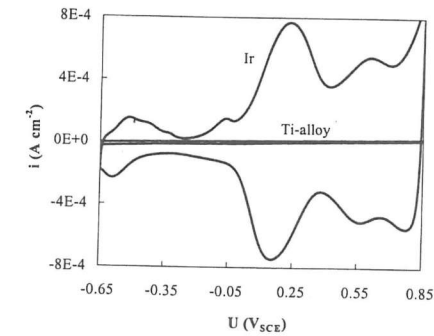


Fig. 2 - Typical voltammograms obtained for pure Ir and for the unimplanted Ti-alloy, after 100 potential cycles.

In Fig. 3, voltammetric plots are shown for the Ir-implanted alloy immersed for several periods in the etching solution. As it can be seen, the voltammetric curves obtained for the implanted samples closely resembles that obtained for the oxide grown on pure iridium, with the characteristic main anodic and cathodic peaks at the same potentials.

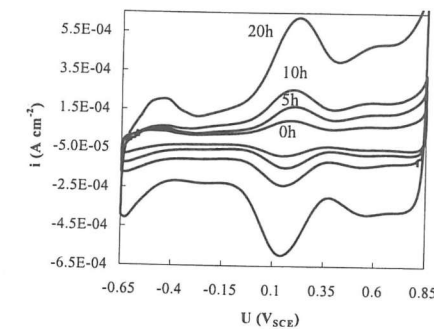


Fig. 3 - Cyclic voltammograms of the chemically etched Ir-implanted samples, after 100 potential cycles (time of etching is indicated in the figure)

The variation of the charge storage capacity, evaluated by integrating under the voltammetric curve, with the etching period presents a peak in the order of  $10\text{mC/cm}^2$  for an immersion period of 20h (Fig. 4). As the charge density is related to the presence of Ir atoms at the surface of the material it can be inferred that the highest surface Ir concentration is obtained for the sample immersed for 20h. Moreover, the similarity in shape of this curve and of the implant profile of Fig.1 suggests that, as consequence of etching in 70%  $\text{H}_2\text{SO}_4$ , the implanted alloy/solution interface progressively moves inwards through the original implant profile. After 20h of immersion in acid the concentration peak of Ir in the SIMS profile is attained.

It should also be noticed that for the 20h immersed samples a charge density of  $10\text{mC/cm}^2$  is achieved, which is considered enough for auditory prostheses.

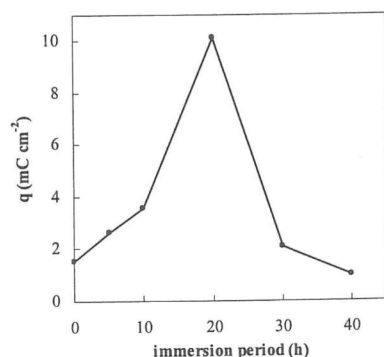


Fig. 4 - Voltammetric charge (measured after 100 potential cycles) for the Ir-implanted electrodes as a function of the etching period.

#### Chemical composition

To confirm whether a displacement of the implanted profile towards the surface occurs as consequence of etching, chemical analysis was performed by AES depth profiling on the oxides formed in two different limiting cases: samples that were etched for 20h and samples that were not submitted to chemical etching (0h of immersion).

One of the limitations of the AES technique is the difficulty in determining the sputtering rate without using standards of known thickness. To avoid this problem AES depth profile was also performed on an as-implanted sample and calibration of the depth scale was made comparing this profile with that obtained by SIMS.

Fig. 5 shows the Ir/Ti ratio as a function of thickness for the three samples. Relatively to the as-implanted sample, a shift in the peak concentration towards the surface is observed for both the 0h and 20h immersion periods. A significant difference is however observed between the surface Ir

concentration of these two last samples.

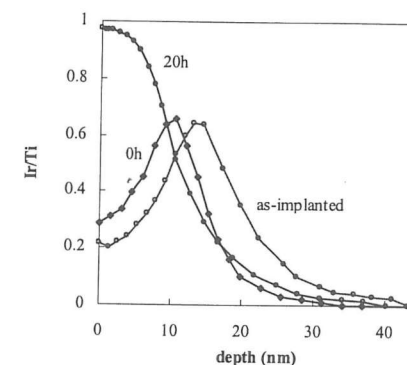


Fig. 5 - Ir/Ti vs. depth, determined by Auger profiling, for the Ir-implanted Ti alloy in three different cases: as received, after 100 potential cycles and after 20h of etching in acid + 100 potential cycles.

As mentioned before, immersion in acid leads to selective dissolution of Ti with accumulation of iridium atoms at the surface. It is therefore expectable that an Ir-rich layer is formed at the surface. On the contrary, for the case of the non-etched sample the raise in the Ir surface concentration can be explained by uniform dissolution of the electrode surface conducting to a displacement of the electrode/solution interface towards a inner Ir-richer region. A similar mechanism has already been proposed by other authors, for Ir and Ru ion implanted in Ti [27,28]. In fact, as determined by XPS [29], anodic oxidation of these implanted materials leads to the formation of a substitutional solid solution,  $\text{M}_x\text{Ti}_{(1-x)}\text{O}_2$  (where M represents the noble metal), at the electrode/solution interface. This mixed oxide dissolves without preferential corrosion of any of the cationic components of the oxide. Similarly Kötzt et al [30] found that  $\text{Ru}_x\text{Ir}_{(1-x)}\text{O}_2$  films, formed by reactive sputtering, corroded in a non-preferential mode, and attributed this observation to the fact that  $\text{Ru}_x\text{Ir}_{(1-x)}\text{O}_2$  is a homogeneous solid solution over the entire range of x.

The fact that the ratio  $\text{O}/(\text{Ti}+\text{Ir})$ , determined by AES measurements, is close to 2 for the immersed samples supports the fact that also in this case a mixed oxide forms at the surface of the samples.

The enhanced charge storage capacity of the 20h immersed sample is therefore related to an increase in Ir surface concentration as a result of two different processes: selective dissolution of the Ti-alloy, occurring during immersion, with consequent build-up of Ir at the surface and uniform dissolution of the mixed oxide leading to the displacement of the original implant profile towards the surface.

Capacitance measurements

Typical Mott-Schottky plots, obtained by ac-measurements, are shown in Fig. 6a for the case of the unimplanted Ti-alloy and in Fig. 6b for the case of pure iridium and of the Ir-implanted samples immersed for different periods.

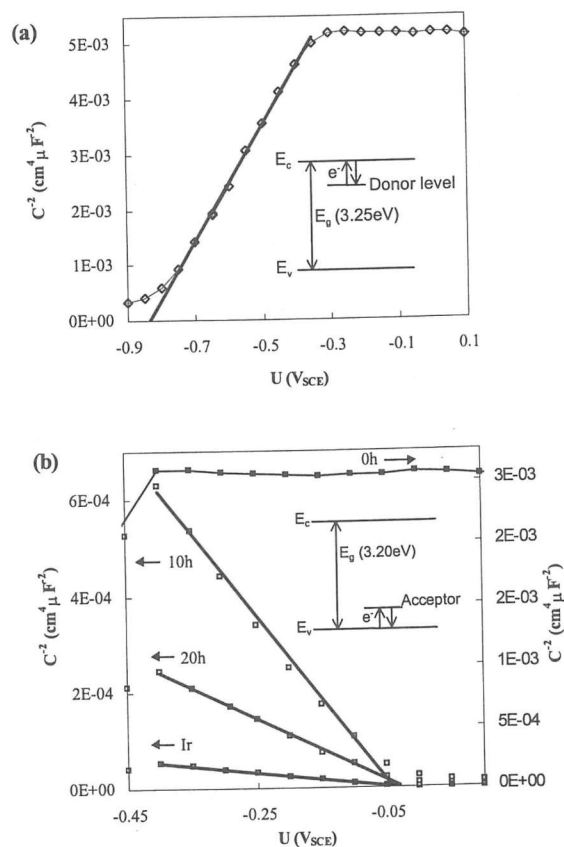


Fig. 6 - Mott-Schottky plots of the oxides formed on (a) the unimplanted Ti-alloy (b) on the Ir-implanted samples etched for different periods, and on a pure Ir substrate.

For the unimplanted Ti-alloy the presence of a straight line presenting a positive slope indicates a n-type semiconducting behaviour. In fact, for the experimental conditions used it is expected that a thin film of TiO<sub>2</sub> cover the Ti-alloy. It is well known that this oxide behaves as n-type semiconductor exhibiting a flatband potential given by  $U_{FB} = -0.35 - 0.059pH$  [31], which is in

good agreement with the value obtained by the intercept of the straight line with the potential axis.

Conversely, for the case of pure Ir electrodes a p-type semiconducting behaviour can be inferred from the negative slope of the Mott-Schottky plot as already described in previous publication [32]. It should also be noticed that, in this case, higher values of capacity are observed related with the high real area due to the hyper-extended surface of these oxides [10,32].

For the case of the electrodes immersed for 10h and 20h a p-type semiconducting behaviour, similar to that of pure iridium oxides can also be observed. In the case of the sample immersed for 0h a different behaviour is observed. The fact that  $C^{-2}$  is constant in the entire potential region indicates a dielectric behaviour

It can therefore be stated that the plots evolve from an n-type semiconductor (typical of Ti oxides) to a p-type semiconductor (typical of Ir oxides) when a sufficient amount of iridium is present at the electrode surface.

The disappearance of the n-type semiconducting behaviour of anodic oxides formed on Ru and Ir implanted Ti electrodes have been studied previously by Vallet et al by means of photoacoustic and photocurrent spectroscopy [33,34]. In these experiments it was found out that the semiconductor absorption bandgap disappeared for Ir/Ti and Ru/Ti ratios lower than 0.1. According to these authors, this insulating/metal transition can not be explained considering a mixture of IrO<sub>2</sub> and TiO<sub>2</sub> oxides. In fact, in this case, the transition would occur for higher levels of noble metal [35], since the iridium oxide phase should form a continuous path across the sample in order to obtain a metallic response. Mixing should therefore take place on an atomic scale. Considering this hypotheses the insulating/metal transition was explained by the formation of localised states in the bandgap, which eventually overlap the conduction band, as Ir(IV) or Ru(IV) is substituting for Ti(IV) [29,35]

In spite of the fact that the crystalline structure of Ti oxides is still controversial, recent studies of thin Ti anodic films [36] show that rutile was the only identifiable phase. Moreover, iridium oxide crystallises (in a microscopic level) with a rutile form. Therefore, the formation of a mixed oxide presenting a rutile-type structure, with Ir substituting for Ti, is likely to occur by oxidation of the implanted alloy.

In this work a different interpretation for the disappearance of the absorption bandgap is put forward. In fact, instead of an insulating/metal transition, a n-type to p-type transition is admitted to occur with increasing content of Ir in the mixed oxide. The fact that no photocurrent response from Ir-implanted electrodes (p-type semiconductor) was detected in Vallet et al work [33] is explained by the fact that these experiments were performed at an applied potential of 1.0V and, in these conditions, degeneration of the semiconductor in the space-charge region exists [32].

The band structure models for TiO<sub>2</sub> and IrO<sub>2</sub> are shown respectively in the inserts of Fig. 6a and 6b. The bandgap energy for these two oxides is very similar [32, 37], supporting the idea of the formation of a mixed oxide.

In the case of TiO<sub>2</sub> the n-type semiconductivity can be related to the presence of interstitial cations, which acts as donor levels (Fig. 6a). Conversely, the p-type semiconductivity displayed by IrO<sub>2</sub> is most probably promoted by cation vacancies, which inject holes in the valence band (Fig. 6b). Because the high doping density the donor and acceptor levels are very close to the conduction and valence bands respectively.

The oxide film formed on the implanted Ti-alloy surface manifests a n-type or a p-type semiconducting behaviour depending on the predominant defects present in the film. It is feasible that the dielectric behaviour for the Oh immersed sample is related to an intermediate situation where both acceptor and donor levels are present in such a concentration that the film behaves as an intrinsic semiconductor, with the Fermi level positioned in the middle of the bandgap.

The capacitance results obtained reflect the existence of two kinds of doping levels. They are also in good agreement with the fact that the oxide films formed on these implanted materials can be considered as a substitutional solid solution type Ir<sub>x</sub>Ti<sub>(1-x)</sub>O<sub>2</sub> [27].

The electronic structure models that can be proposed according to the p-type or n-type semiconducting behaviour of these two oxides are also in agreement with their voltammetric response. In fact, the low charge storage capacity presented by the n-type oxides formed on Ti-alloy can be related to upwards band bending at the oxide/electrolyte interface as consequence of electrode polarisation at U>U<sub>b</sub> (-0.8V). In these circumstances, formation of a depleted space-charge layer occurs and the low concentration of electrons in the conduction band inhibits all faradaic processes (Fig. 7a).

On the other hand, since iridium oxide presents a p-type behaviour the upward band bending (occurring in this material for U>0V) leads to an accumulation layer. Because a sufficiently high concentration of holes is present in the valence band, the Ir(III)/Ir(IV) transition, which is mainly responsible for charge storage at this oxide, can readily occur (Fig. 7b).

**Conclusions**

Production of neuro-stimulating electrodes, presenting good electrochemical properties and enhanced mechanical behaviour, is possible by ion implantation of Ir into Ti-6Al-4V alloy followed by an appropriate chemical etching.

Auger depth profiling of the surface oxides revealed that the enrichment of Ir at the surface is a result of the combined effect of uniform dissolution of the mixed oxide and of preferential dissolution

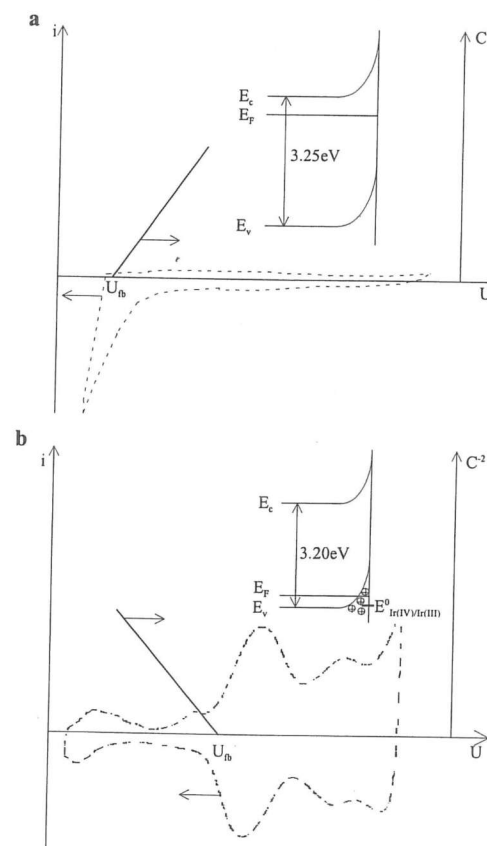


Fig. 7 - Voltammograms, Mott-Schottky plots and schematic representation of the band diagram valid when U>U<sub>b</sub> for a) TiO<sub>2</sub> and b) IrO<sub>2</sub>

of the Ti-alloy as consequence of etching in acid.

It was shown by capacitance measurements that the oxide films formed on the Ir-implanted Ti-alloy exhibit a transition from a n-type to a p-type semiconducting behaviour with increasing Ir content on the oxide. These results support the formation of a mixed oxide where Ir(IV) substitutes Ti(IV) in a rutile-like structure.

### References

1. F. T. Hambrecht, *Mat. Res. Symp. Proc.*, **55** (1986) 265
2. J. McHardy, L. S. Robblee, J. M. Marston and S. B. Brummer, *Biomaterials*, **1** (1980) 129
3. P. K. Campbell and K. E. Jones in "Materials Science and Technology" vol. 14 D. F. Williams Vol. Ed. VCH Publishers Inc., NY (1992)
4. I. S. Lee, R. A. Buchanan and J. M. Williams, *J. Biomed. Mat. Res.*, **25** (1991) 1093
5. S. B. Brummer and J. M. Truner, *IEEE Trans. Biomed. Eng.*, **24** (1977) 59
6. L. S. Robblee, J. L. Lefko and S. B. Brummer, *J. Electrochem. Soc.*, **130** (1983) 731
7. L. S. Robblee, M. J. Michael, J. Mangaudis, E. D. Lasinsky A.G. Kimbala and S. B. Brummer *Mat. Res. Soc. Symp. Proc.*, **55** (1986) 303
8. S. Gottesfeld and S. Srinivasan, *J. Electroanal. Chem.*, **86** (1978), 89
9. V. Birss, R. Myers, H. Angerstein-Kozłowska and B. E. Conway, *J. Electrochem. Soc.*, **131** (1984), 1502
10. B. E. Conway and J. Mozota, *Electrochem. Acta*, **28** (1983) 9
11. J. D. E. McIntyre, W. F. Peck Jr. and S. Nakahara, *J. Electrochem. Soc.*, **127** (1980) 1264
12. S. Gottesfeld and J. D. E. McIntyre, *J. Electrochem. Soc.*, **126** (1979) 742
13. L. D. Burke and R. A. Scannell, *J. Electroanal. Chem.*, **175** (1984) 119.
14. L. D. Burke and D. P. Whelan, *J. Electroanal. Chem.*, **162** (1984) 121
15. G. Beni, C. E. Rice and J. L. Shay, *J. Electrochem. Soc.*, **127** (1988) 1342
16. N. Buckley and L. D. Burke, *J. Chem. Soc., Faraday Trans. 1*, **71** (1975) 1447
17. G. Beni and J. L. Shay, *Phys. Rev. B.*, **21** (1980) 364
18. S. H. Glarum and J. H. Marshall, *J. Electrochem. Soc.*, **127** (1980) 1467
19. T. M. Silva, J. E. Rito, A. M. P. Simões, M. G. S. Ferreira, M. da Cunha Belo and K. G. Watkins, *Electrochem. Acta*, **43** (1997), 203
20. G. K. Hubler and E. McCafferty, *Corros. Sci.*, **20** (1980) 103
21. M. Stern and H. Wissenbergm, *J. Electrochem. Soc.*, **106** (1959) 759
22. O. Zabrino, N. R. de Tacconi and A. J. Arvia, *J. Electrochem. Soc.*, **125** (1978) 1266
23. P. G. Pickup and V. I. Birss, *J. Electroanal. Chem.*, **240** (1988) 185
24. G. Beni and J. L. Shay, "Fast Ion Transport in Solids", Vashita, Mundy, Shenoy eds., Elsevier (1979) 75
25. L. M. Schiavone, W. C. Dautremont-Simth, G. Beni and J. L. Shay, *J. Electrochem. Soc.*, **128** (1981) 1339
26. C. Guttierrez, M<sup>a</sup> Sanchez, J. I. Peña, C. Martínez and M. A. Martínez, *J. Electrochem. Soc.*, **134** (1987), 2119

27. E. J. Kelly, C. E. Vallet and C. W. White, *J. Electrochem. Soc.*, **137** (1990) 2482
28. E. J. Kelly, D. E. Heatherly, C. E. Vallet and C. W. White, *J. Electrochem. Soc.*, **134** (1987) 1667
29. C. E. Vallet, A. Choudhury, P. E. Sobol and C. W. White, *Electrochem. Acta*, **38** (1993) 1313
30. R. Kötz and S. Stucki, *Electrochem. Acta*, **31** (1986) 1311
31. M. Tomkiewicz, *J. Electrochem. Soc.*, **126** (1979) 1505
32. T. M. Silva, A. M. P. Simões, M. G. S. Ferreira, M. Walls and M. da Cunha Belo, *J. Electroanal. Chem.*, **441** (1998) 5
33. C. E. Vallet, D. E. Heatherly, and C. W. White, *J. Electrochem. Soc.*, **137** (1990) 579
34. C. E. Vallet, S. E. Borns, J. S. Hendrickson and C. W. White, *J. Electrochem. Soc.*, **135** (1988) 387
35. C. E. Vallet, *J. Electrochem. Soc.*, **138** (1991) 1234
36. M. R. Kozłowski, P. S. Tyler, W. H. Smyrl and R. T. Atanasoski, *J. Electrochem. Soc.*, **136** (1988) 442
37. S. Piazza, L. Calà, C. Sunseri and F. Di Quarto, *Ber. Bunsenges. Phys. Chem.*, **101** (1977) 932

Received, July 12, 1998  
Accepted, September 21, 1998